Rheumatology, 2024, **00**, 1–8
https://doi.org/10.1093/rheumatology/keae577
Advance access publication 22 November 2024
Original Article

Clinical science

^{68}Ga-FAPI and ^{18}F-NaF PET/CT in psoriatic arthritis: a comparative study

Fan Yang [1,2], Chaofan Lu[1], Qingqing Pan[3], Rui Zhang[4], Meng Yang[4], Qian Wang [1], Mengtao Li [1], Xiaofeng Zeng [1], Yaping Luo[3,5,*], Xiaomei Leng[1]

[1]Department of Rheumatology and Clinical Immunology, Peking Union Medical College Hospital, Chinese Academy of Medical Sciences & Peking Union Medical College, National Clinical Research Center for Dermatologic and Immunologic Diseases (NCRC-DID), Key Laboratory of Rheumatology and Clinical Immunology, Ministry of Education, Beijing, China
[2]Department of Rheumatology, Beijing Friendship Hospital, Capital Medical University, Beijing, China
[3]Department of Nuclear Medicine, Chinese Academy of Medical Sciences and Peking Union Medical College Hospital, Beijing, China
[4]Department of Ultrasonography, State Key Laboratory of Complex Severe and Rare Diseases, Peking Union Medical College Hospital, Chinese Academy of Medical Sciences and Peking Union Medical College, Beijing, China
[5]State Key Laboratory of Common Mechanism Research for Major Diseases, Beijing, China

*Correspondence to: Yaping Luo and Xiaomei Leng, Peking Union Medical College Hospital (PUMCH), No. 1 Shuaifuyuan, Wangfujing Ave, Beijing 100730, China. E-mail: luoyaping@live.com; lpumch@126.com

Abstract

Objectives: As fibroblast-like synoviocyte activation and bone formation are associated with PsA, PET using the tracers of ^{68}Ga-fibroblast activation protein inhibitor (FAPI) and ^{18}F-sodium fluoride (NaF) may sensitively detect the disease. In this prospective study, we aimed to evaluate the performance of ^{68}Ga-FAPI PET/CT in PsA and to compare it with ^{18}F-NaF PET/CT.

Methods: Sixteen participants (female 7/16, age 42.31 ± 10.66 years) with PsA were prospectively enrolled and underwent dual-tracer PET/CT, clinical assessment and ultrasonography. PET/CT images were scored for PET-positive lesions at the peripheral joints, entheses, and axial joints.

Results: The positivity rate of ^{68}Ga-FAPI in peripheral joints was higher than that in entheses and axial joints (21.84% *vs* 12.15% *vs* 0%), whereas high positivity rates of ^{18}F-NaF in peripheral joints, entheses, and axial joints were observed (85.23%, 78.13% and 75%, respectively). The DAS 28 was higher in the PET-positive than in the PET-negative group with ^{68}Ga-FAPI (5.25 ± 1.84 *vs* 2.55 ± 0.94, $P = 0.037$), but not with ^{18}F-NaF. In addition, the PET joint count at ^{68}Ga-FAPI PET/CT was positively correlated with the tender joint count ($r = 0.604$, $P = 0.017$), swollen joint count ($r = 0.773$, $P = 0.001$), DAS28-CRP ($r = 0.556$, $P = 0.032$), Psoriatic Arthritis Disease Activity Score (PASDAS) ($r = 0.540$, $P = 0.038$) and PsASon13 ($r = 0.701$, $P = 0.005$), while no correlation was observed in ^{18}F-NaF PET/CT.

Conclusion: The positivity rates of ^{68}Ga-FAPI- and ^{18}F-NaF PET/CT were different in patients with PsA in peripheral joints, entheses, and axial joints. The extent of joint involvement as shown in ^{68}Ga-FAPI PET/CT correlated with clinical and US variables as well as with disease activity.

Trial registration: ClinicalTrials.gov, http://clinicaltrials.gov, NCT05686876.

Keywords: fibroblast activation protein, oositron emission tomography/computed tomography, psoriatic arthritis.

Rheumatology key messages

- The positivity rates of ^{68}Ga-FAPI and ^{18}F-NaF PET/CT differed in entheses, peripheral and axial joints.
- The positivity rate of ^{68}Ga-FAPI was higher in peripheral joints than in entheses and axial joints.
- The extent of joint involvement as shown in ^{68}Ga-FAPI PET/CT correlated with disease activity, but not as shown in ^{18}F-NaF.

Introduction

PsA is a chronic inflammatory disease characterized by diverse clinical features, including peripheral arthritis, enthesitis, axial arthritis, dactylitis, and nail dystrophy, which present either alone or in combination [1]. Inflammation of the synovial membranes and entheseal sites, the main features of PsA, leads to pain, structural damage, impairment of physical function, and poor quality of life [2]. Axial involvement is a key clinical feature of PsA [3]. Similar to other forms of inflammatory arthritis, abrogation of inflammation is a central goal in PsA treatment. However, PsA is heterogeneous in nature, with an array of symptoms and effects, posing challenges in its diagnosis and treatment [4].

Clinical assessment of PsA has limited accuracy, because it is based only on the presence of soft tissue tenderness and swelling. Advanced imaging techniques, such as US and MRI have shown promise for the sensitive detection of musculoskeletal inflammation. However, these techniques also have

Received: 30 January 2024. **Accepted:** 8 October 2024

shortcomings, like being time-consuming and prone to inter-observer variability [5]. PET allows for a highly sensitive description of targets at a molecular level and can be used to visualize cells of interest by means of specific tracers [6]. More importantly, the entire body can be visualized in a single imaging session.

Given that the inflammatory proliferative cascade in PsA involves cellular activation, angiogenesis, and osteoclastic and osteoblastic activity, targeted radiotracers can be employed to track disease [2]. Fibroblast-like synoviocytes (FLS) play a central role in the pathogenesis of PsA, and fibroblast activation protein (FAP), which is highly expressed in FLS in synovial tissues, is considered a specific marker of FLS activation [7, 8]. We had previously confirmed this in unpublished work on FAP expression in PsA (Supplementary Fig. S1, available at *Rheumatology* online). Dorst *et al.* identified the feasibility of using a radiolabelled anti-FAP antibody to image activated FLS in a mouse model of collagen-induced arthritis [9, 10]. A previous study determined the performance of gallium 68 (^{68}Ga)-labelled FAP inhibitor (FAPI) in assessing joint disease activity in RA [11]. These studies confirm the role of FAP in synovitis and support the approach of FAP-targeted imaging in participants with PsA. To date, only one study using the tracer of ^{68}Ga-FAPI has been published as an abstract, and it showed that fibroblast activation is correlated with disease progression and joint damage in PsA [12].

Fluorine 18-labelled sodium fluoride (^{18}F-NaF) can depict new bone formation resulting from osteoblastic activity [13]. Since enthesitis and axial PsA can be accompanied by bone formation, ^{18}F-NaF PET may enable sensitive detection in these regions [14]. In addition, a previous study found that ^{18}F-NaF accumulated in erosive bone lesions of joints with synovitis, and increased ^{18}F-NaF uptake was associated with progressive joint damage [15]. Jongh *et al.* recently revealed that ^{18}F-NaF PET/CT could sensitively depict the bone turnover at peripheral and axial sites [16].

Since ^{68}Ga-FAPI PET/CT could evaluate the synovial inflammation contributed by FLS, and ^{18}F-NaF PET/CT could depict the new bone formation at joints and entheses, the purpose of our study was to evaluate the performance of ^{68}Ga-FAPI PET/CT in patients with PsA and to explore the extent of FLS' involvement, then to compare it with ^{18}F-NaF PET/CT, which served as a reference.

Methods

This study was approved by the Institutional Review Board of the Peking Union Medical College Hospital (Clinicaltrials.gov: NCT05686876). Written informed consent was obtained from all the participants.

Sixteen patients with PsA who fulfilled the 2006 Classification Criteria for Psoriatic Arthritis (CASPAR) were consecutively recruited from the Department of Rheumatology of Peking Union Medical College Hospital between June 2021 and February 2023 [17]. Patients with known malignancies or autoimmune disorders were excluded. We evaluated all patients using whole-body ^{18}F-NaF and ^{68}Ga-FAPI PET/CT scans, with both scans performed within 1 week. One of the enrolled participants did not complete the ^{18}F-NaF PET/CT and the other did not complete the ^{68}Ga-FAPI PET/CT, both for personal reasons. Patients underwent clinical, ultrasonographic, and SI joint CT evaluations at enrolment. After imaging, all participants underwent secukinumab treatment. Three patients then underwent follow-up clinical examinations and dual-tracer PET/CT scans 6 months after the initial evaluation.

Clinical assessments

Patients were clinically assessed by two experienced rheumatologists according to a standardized protocol that included obtaining demographic information and history of disease duration. The physical examination included assessment of 76 joints (e.g. bilateral temporomandibular joints, sternoclavicular joints, acromioclavicular joints, shoulders, elbows, wrists, MCP joints, MTP joints, PIP joints of the hands and feet, DIP joints of the hands and feet, hips, knees, ankles, and midtarsal joints), entheseal sites included in spondyloarthritis research consortium of Canada (SPARCC), Maastricht Ankylosing Spondylitis Enthesitis Score (MASES) and Leeds enthesitis index (LEI) (bilateral supraspinatus insertion, lateral and medial epicondyles, greater trochanter, quadriceps insertion, inferior patella, tibial tubercle, achilles tendon insertion, plantar fascia insertion, medial femoral condyles, the first and seventh costochondral joints, posterior superior iliac spines, anterior superior iliac spines, iliac crests, and the fifth lumbar spinous process), inflammatory back pain, and the Psoriasis Area and Severity Index. The latter is a measurement of the discoloration, thickness, scaling, and coverage of psoriasis plaques. Laboratory parameters, such as CRP level and ESR, were also determined. The composite indices for disease activity assessment were calculated, including the disease activity index for psoriatic arthritis (DAPSA) score [a numerical sum of tender joint count (TJC), swollen joint count (SJC), patient global assessment, and CRP level), the DAS using 28-joint counts with CRP (DAS28-CRP) and the psoriatic arthritis disease activity score (PASDAS) (a PsA-specific composite measure including the physician and patient global disease activity visual analogue score, the physical component score of the short-form 12, SJC, TJC, Leeds Enthesitis Index, dactylitis count, and CRP).

Ultrasonography and SI joint CT

All US examinations were performed using commercially available ultrasonic equipment (Resona 7, Mindray Bio-Medical Electronics Co. Ltd Shenzhen, China), equipped with a handheld linear L20-5U probe operating at a central frequency of 12.9 MHz. Sixteen joints and 14 entheses were examined in each patient using gray-scale and power Doppler ultrasonography. The evaluated joints included the wrist; MCP2-3 joints, MCP5 joint, PIP1-3 joints, and DIP2-3 joints of the hand; the knee; and MTP1-2 joints, MTP5 joint, IP1 joint, and DIP2–3 joints of the feet on the dominant site. The evaluated entheses included the bilateral supraspinatus insertion, Achilles tendon insertion, plantar fascia insertion, distal patellar ligament enthesis, proximal patellar ligament enthesis, quadriceps tendon insertion, and triceps tendon insertion. Moreover, the PsA US composite scores and Madrid Sonographic Enthesis Index, which reflect synovitis and enthesitis, respectively, were recorded [18, 19]. The US readers were blinded to the clinical and PET/CT data of the patients.

Dedicated SI joint CT scans were obtained using an Aquilion One Imager (Toshiba, Minato, Japan). The acquisition parameters were as follows: field-of-view, 12 cm; acquisition matrix size, 512 × 512 pixels; tube voltage 120–130 kV; tube current, 200 mA; rotation time, 0.75 s; axial slice thickness, 0.5 mm; and interslice gap, 0.25 mm. Morphological assessment of the SI joint was performed on 30 semi-coronal

reconstructions without a gap, with a slice thickness of 1.5 mm and a bone filter.

PET/CT scan and image interpretation

We used 1,4,7,10-tetraazacyclododecane-1,4,7,10-tetraacetic acid, or DOTA, FAPI-04 peptide (CSBio, Menlo Park, CA). ^{68}Ga-FAPI was manually radiolabelled before injection, as described by Luo *et al.* [20]. ^{18}F-NaF was synthesized in-house using an 11-MeV cyclotron (CTI RDS 111; Siemens, Munich, Germany). PET scans were performed using a dedicated Biograph 64 TruePoint TrueV (Siemens) and a Polestar m660 (Sino Union, Beijing, China). For ^{68}Ga-FAPI PET/CT, imaging was performed (2 min per bed) with an uptake time of 68.00 ± 21.23 min after an injection of 3.15 ± 1.15 mCi ^{68}Ga-FAPI. In addition, an injection of ^{18}F-NaF (0.1 mCi per kilogram of body weight) was injected intravenously and the PET/CT images (2 min per bed) were acquired with an uptake time of 106.13 ± 22.67 min. An unenhanced low-dose CT scan (120 kV, 30–50 mAs) was obtained prior to each PET scanning, and used for attenuation correction and anatomic information of the PET images. The scanning time for each PET/CT was 20 min. The acquired data were reconstructed using an ordered subset expectation–maximization method.

PET/CT images were transferred to a Siemens multimodality workstation and were visually assessed by two nuclear medicine physicians. These two nuclear medicine physicians, each with >10 years of experience in PET/CT, worked together to assess the PET/CT images in a random order. Readers were blinded to the clinical data, except PsA diagnosis, and performed a consensus image interpretation. All foci of increased uptake in the peripheral joints, entheses, and axial skeleton were described.

Clinically, joint involvement in PsA refers to tender or swollen joints observed on physical examination by senior rheumatologists, or evidence of synovitis on imaging. Similarly, enthesis involvement refers to a tender enthesis on physical examination, or evidence of enthesitis on imaging. On PET/CT, a PsA-positive joint or enthesis was defined as increased articular or entheseal radioactivity as compared with background uptake. The PsA-positive joints and entheses detected on either ^{18}F-NaF or ^{68}Ga-FAPI PET/CT were analysed individually. The number of PsA-positive joints on PET was recorded as the PET joint count and the number of enthesis-positive entheses as the PET enthesis count. Clinically, axial involvement was defined as the abnormal imaging examinations (X-ray and CT) of spine or SI joint. On PET/CT, axial involvement was defined as high uptake at the spine and SI joints.

Statistical analysis

Categorical variables are described as frequencies and percentages and quantitative variables as means and S.D.s or medians and interquartile ranges. Descriptive data were compared between groups using Student's *t* test or the Mann–Whitney *U* test. Cohen's kappa test was used to calculate consensus agreement for PET/CT, physical exam and US. Spearman's rank correlation test was used to evaluate correlations of PET data with clinical and US data. Sensitivity and specificity were analysed by a Receiver Operating Characteristic (ROC) curve. For correction of multiple comparisons, the Benjamini–Hochberg method was performed to control the rates of false-positive findings. Statistical significance was set at $P < 0.05$. All statistical analyses were performed using SPSS (version 24.0; IBM Corp., Armonk, NY).

Results

Patients

Sixteen participants with PsA (nine men and seven women; 42.31 years ± 10.66) were enrolled in this prospective study. The patients had a median disease duration of 91.5 months (range, 1–400 months). The clinical characteristics of the patients are summarized in Table 1 (and the follow-up information is included in Supplementary Table S1 and Fig. S2, available at *Rheumatology* online). The images of both the axial and peripheral skeletons were of good quality for identifying PET-positive lesions.

Peripheral joints

^{18}F-NaF PET/CT was visually positive for peripheral arthritis in all patients with PsA (100%), whereas ^{68}Ga-FAPI PET/CT was positive in 8 of the 15 patients (53.33%) (Figs 1, 2). ^{18}F-NaF uptake was observed in 277 of the 1064 joints (26.03%), while tracer uptake on ^{68}Ga-FAPI scans was observed in 71 joints (6.67%). Among them, 58 joints were positive on both PET/CT examinations, 13 (1.22%) FAPI-avid joints were not detected on ^{18}F-NaF PET/CT, and 219 (20.58%) were missed on ^{68}Ga-FAPI PET/CT. Eighty-nine tender or swollen joints were identified during physical examination. When combining physical examination and PET/CT, a total of 325 joints were found to be involved. Therefore, the positivity rates of detecting involved joints were 27.38% (89/325) for physical examination, 21.84% (71/325) for ^{68}Ga-FAPI PET/CT, and 85.23% (277/325) for ^{18}F-NaF PET/CT (according to the calculation method of Luo *et al.*) [11].

US revealed 85 positive findings. Among them, 22.35% (19/85) of the US-positive joints were clinically positive.

Table 1. Baseline characteristics of the enrolled patients

Parameter	Value
Age (years)	42.31 ± 10.66
Sex (male/female)	9/7
Disease duration (years)	7.81 ± 8.65
TJC76, median (IQR)	2.5(5)
SJC74, median (IQR)	1.5(3.5)
SPARCC, median (IQR)	0 (0,5)
MASES, median (IQR)	0 (0,2)
LEI, median (IQR)	0 (0,10)
IBP, *n* (%)	8 (50.0)
PASI	6.89 ± 11.77
Axial involvement, *n* (%)	10 (62.5)
Peripheral erosion, *n* (%)	5 (31.3)
ESR (mm/h)	19.56 ± 19.81
CRP (mg/dl)	8.42 ± 11.62
DAPSA	22.42 ± 24.68
DAS28-CRP	2.82 ± 1.26
PASDAS	3.96 ± 1.73
PsASon13	20.07 ± 20.03
MASEI	13.79 ± 17.89
Treatment	
NSAIDs, *n* (%)	4 (25.0)
MTX, *n* (%)	4 (25.0)
TNFi, *n* (%)	3 (18.8)

TJC: tender joint count; SJC: swollen joint count; SPARCC: spondyloarthritis research consortium of Canada; MASES: Maastricht Ankylosing Spondylitis Enthesitis Score; LEI: Leeds enthesitis index; IBP: inflammatory back pain; PASI: Psoriasis Area and Severity Index; DAPSA: Disease Activity in Psoriatic Arthritis; DAS28-CRP: DAS 28-CRP; PASDAS: psoriatic arthritis disease activity score; PsASon13: PsA US composite score; MASEI: the Madrid Sonographic Enthesis Index; TNFi: TNF inhibitor.

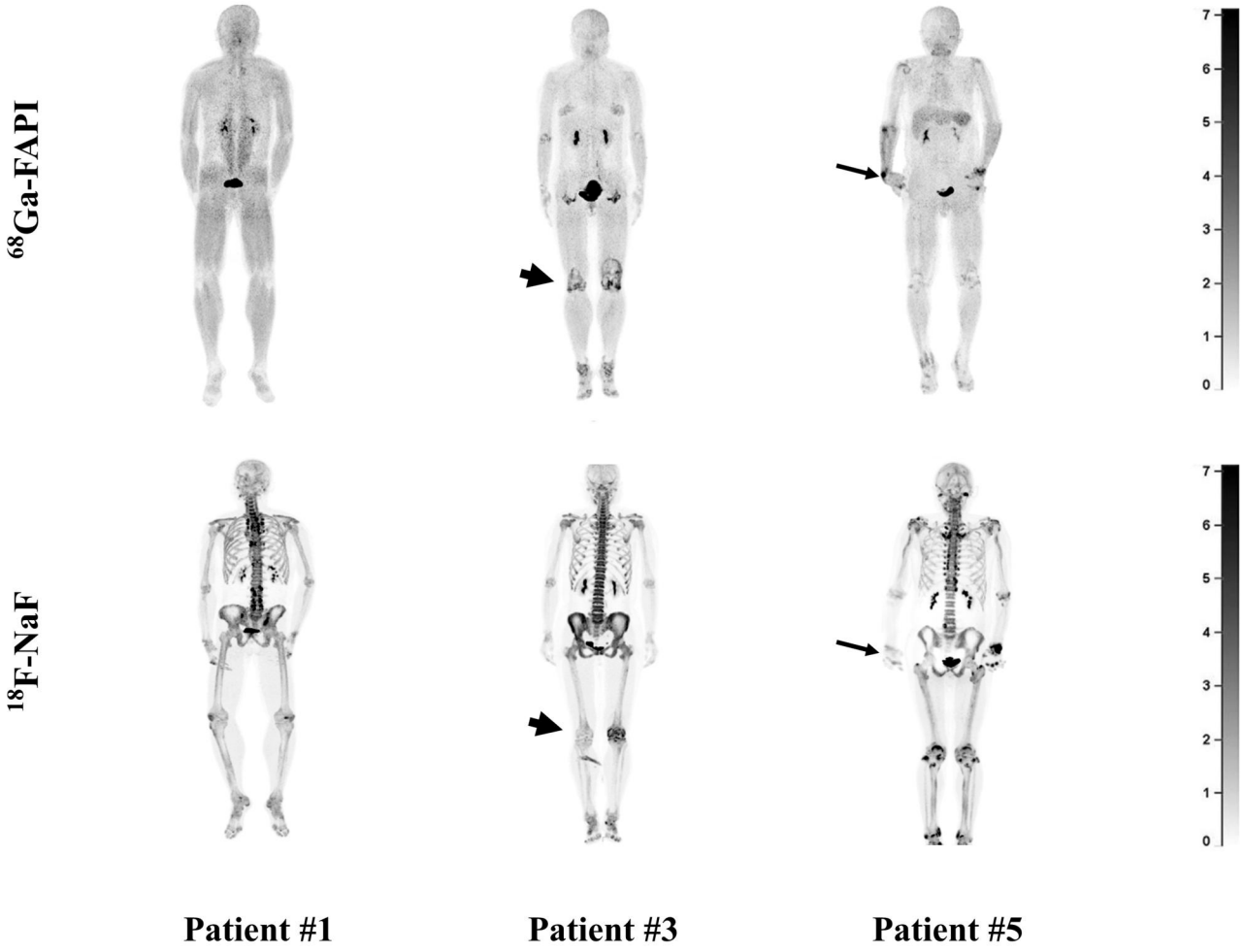

Figure 1. Individual comparison of three participants with PsA undergoing ^{68}Ga FAPI and fluorine ^{18}F-NaF PET/CT. Different uptake patterns of ^{68}Ga-FAPI and ^{18}F-NaF are shown. The uptake intensity of ^{68}Ga-FAPI was higher than that of ^{18}F-NaF PET/CT in the arthritic joints (participants 3 and 5; arrows)

Fifteen joints (17.65%) had positive findings on both US and ^{68}Ga-FAPI PET/CT, whereas two joints (2.35%) were not positive on US but were detected on ^{68}Ga-FAPI PET/CT. For ^{18}F-NaF PET/CT, 64.71% (55/85) of the PET-positive joints were US-positive and 15 (17.65%) were US-negative. The ROC curve, sensitivity, specificity, and AUC values are shown in Supplementary Table S2 and Fig. S3, available at *Rheumatology* online.

The DAS28-CRP score was higher in the PET-positive than in the ^{68}Ga-FAPI PET-negative group [5.25 ± 1.84 *vs* 2.55 ± 0.94, respectively ($P = 0.037$)]. Comparisons were not made for ^{18}F-NaF PET/CT, as all patients had positive findings. Furthermore, using US as standard, the TJC [13.4 ± 13.18 *vs* 1.88 ± 1.64, respectively ($P = 0.019$)], SJC [11.2 ± 12.19 *vs* 0.88 ± 1.25, respectively ($P = 0.006$)], synovitis score on US [37.40 ± 22.23 *vs* 10.63 ± 9.96, respectively ($P = 0.011$)], and proportion of treatment-naive patients [80% *vs* 12.5%, respectively ($P = 0.019$)] was higher in the ^{68}Ga-FAPI PET-positive than in the PET-negative group. No differences were observed in the ^{18}F-NaF scans.

Entheses

Seven of the 15 patients (46.67%) showed ^{18}F-NaF PET/CT enhancement, while three (20.0%) showed ^{68}Ga-FAPI uptake at one or more enthesis sites. In total, 25 of 294 (8.50%) evaluated entheses were ^{18}F-NaF PET-positive, while ^{68}Ga-FAPI uptake was detected in four (1.36%) enthesis sites. No enthesis was found to be involved using both tracers. Four tender entheseal sites (1.36%) were identified upon physical examination. When the physical examination and PET/CT were combined, 32 involved entheses were found. Therefore, the positivity rates were 12.15% (4/32) on physical examination, 12.15% (4/32) on ^{68}Ga-FAPI PET/CT, and 78.13% (25/32) on ^{18}F-NaF PET/CT.

Fifty-three entheses were positive on US. Among them, 3.78% (2/53) of the US-positive joints were clinically positive. One (1.89%) of the US-positive entheses was also ^{68}Ga-FAPI PET/CT-positive, and five (9.43%) were US-negative. For ^{18}F-NaF PET/CT, 28.3% (15/53) entheses were both US- and PET/CT-positive, whereas four (7.55%) were not positive on US but were detected on ^{18}F-NaF PET/CT. The agreements between PET/CT, clinical and US data are summarized in Supplementary Table S3, available at *Rheumatology* online.

Axial joints

Eight of the 15 patients (53.3%) showed ^{18}F-NaF uptake, while none of the patients (0%) showed ^{68}Ga-FAPI uptake at the axial level. Sixty-six of ^{18}F-NaF PET/CT-positive lesions were

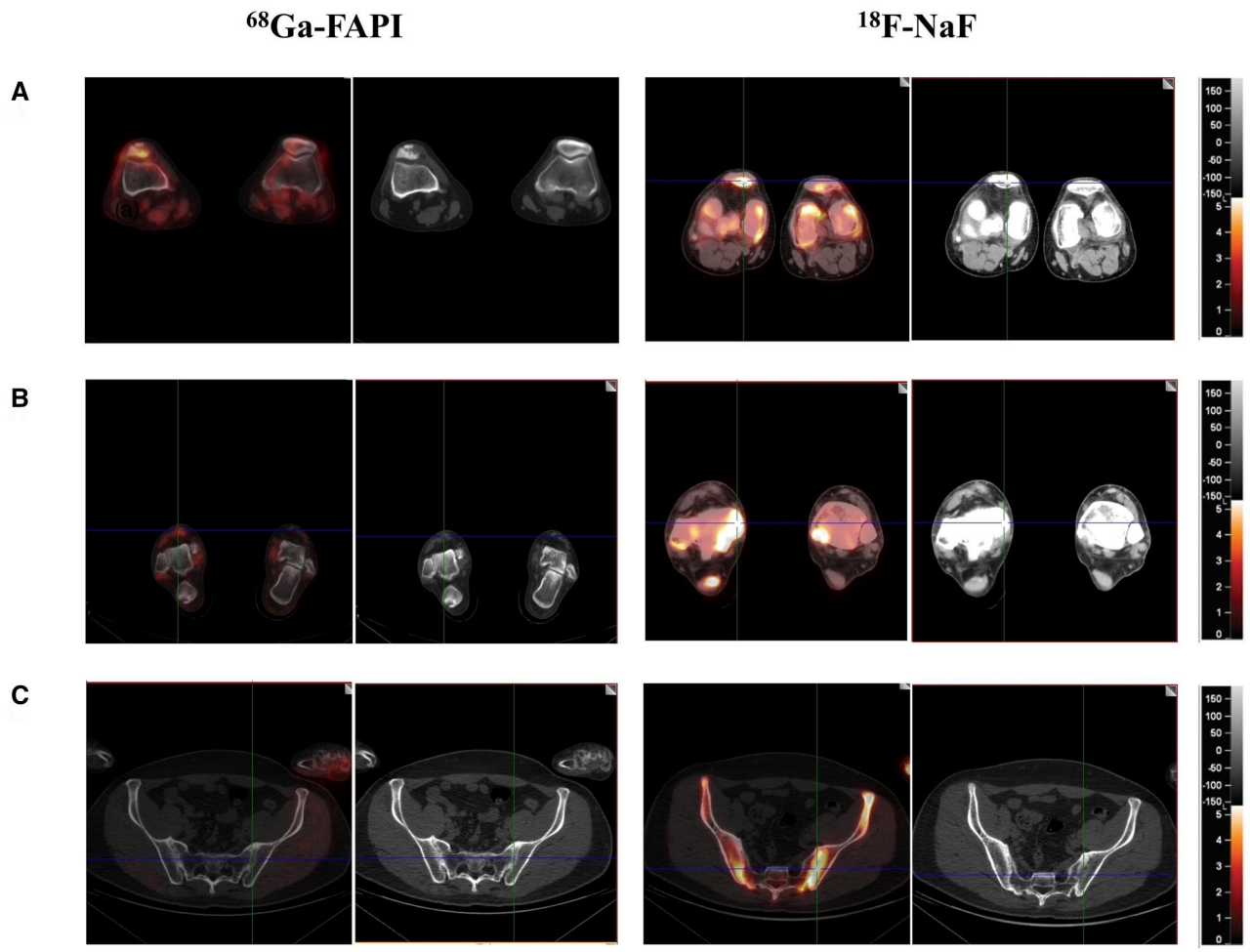

Figure 2. ^{68}Ga-FAPI and ^{18}F-NaF fusion (left side) and co-registered CT images (right side) in patient #5, who is a 65-year-old man with a 31-year history of PsA. (A) Moderate-to-intense uptake of both tracers in the right knee joint. (B and C) Higher uptake intensity of ^{18}F-NaF than that of ^{68}Ga-FAPI PET/CT in the Achilles tendon insertion and SI joints

found in the spine, most frequently in the thoracic vertebrae (57.58%, 38/66), followed by the cervical (36.36%, 24/66), and lumbar vertebrae (6.06%, 4/66). Additionally, PET enhancement was observed in 23.33% (7/30) SI joints. Among the seven PET-positive SI joints, all were positive on SI joint CT scans.

Correlation between PET-derived parameters and clinical and US data

Quantitative PET/CT variables as shown in both ^{68}Ga-FAPI and ^{18}F-NaF PET/CT and clinical and US data are in Table 2 and Supplementary Table S4, available at *Rheumatology* online. The PET joint count at ^{68}Ga-FAPI PET/CT was positively correlated with the TJC ($r = 0.604$, $P = 0.017$), SJC ($r = 0.773$, $P = 0.001$), DAS28-CRP ($r = 0.556$, $P = 0.032$), PASDAS ($r = 0.540$, $P = 0.038$) and PsASon13 ($r = 0.701$, $P = 0.005$). However, there was no correlation between the PET joint count and clinical or US data in ^{18}F-NaF PET/CT.

Discussion

PsA is a heterogeneous disease involving multiple potential tissue domains. Several studies have reported the clinical values of ^{18}F-FDG and ^{18}F-NaF PET/CT in PsA. Abdelhafez *et al.* assessed the performance of ultra-low-dose total-body ^{18}F-FDG PET/CT in patients with PsA and found that systemic joint evaluation is feasible [21]. ^{68}Ga-FAPI is a recently introduced PET agent targeting FAP, a type II transmembrane serine protease. It can be used for imaging different types of cancers and non-malignant diseases [22]. In this study, using ^{18}F-NaF PET/CT, ultrasonography and SI joint CT as references, we evaluated the performance of ^{68}Ga-FAPI PET/CT in patients with PsA.

Table 2. Correlation between PET- derived parameters and clinical and US data

Parameter	^{18}F-NaF PET/CT		^{68}Ga-FAPI PET/CT	
	r	*P*	*r*	*P*
TJC	0.207	0.477	0.604	0.017*
SJC	0.302	0.294	0.773	0.001*
ESR	−0.068	0.816	0.062	0.825
CRP	0.487	0.078	0.095	0.737
DAPSA	0.454	0.103	0.457	0.087
PASDAS	0.513	0.050	0.540	0.038*
DAS28-CRP	0.473	0.088	0.556	0.032*
PsASon13	0.482	0.095	0.701	0.005*

* Significant *P*-value after multiple comparison correction.
TJC: tender joint count; SJC: swollen joint count; DAPSA: Disease Activity in Psoriatic Arthritis; PASDAS: psoriatic arthritis disease activity score; DAS28-CRP: DAS 28-CRP; PsASon13: PsA US composite score.

We found a higher ^{68}Ga-FAPI-positivity rate in peripheral joints than in entheses and axial joints (21.84% *vs* 12.15% *vs* 0%) in patients with PsA. A previous study had shown that inflamed synovia can be visualized using an FAP-targeting tracer [23]. Dorst *et al.* demonstrated that anti-FAP-targeted photodynamic therapy potently induced cell death in synovial fibroblasts of RA patients [23]. PsA synovial fibroblasts can induce angiogenesis, promoting a more dysregulated endothelial cell phenotype than that seen in RA [24]. Therefore, our study supports the role of FAP in PsA peripheral synovitis from a PET/CT perspective. Moreover, it is noted that no axial joint with ^{68}Ga-FAPI was detected, though previous study has reported increased ^{68}Ga-FAPI uptake in the axial joints in RA and AS [11, 25]. The FLS may have distinct pathogenetic mechanisms in PsA and other arthritis. In addition, the PET systems may have lower spatial resolution, and partial voluming may have obscured the findings.

In contrast, high ^{18}F-NaF-positivity rates in peripheral joints, entheses, and axial joints were observed (85.23%, 78.13% and 75%, respectively). Entheses are the initial sites of inflammation in PsA, which then extends to the synovial lining [26]. Enhanced bone formation is associated with entheseal and synovial pathologies in patients with PsA. Syndesmophytes, a radiographic hallmark of SpA, represent bone formation at the margins of vertebral bodies via endochondral ossification [27]. Similar to our results, Jongh *et al.* demonstrated that ^{18}F-NaF PET/CT could detect new bone formation at the peripheral joints, entheses, and axial joints [16]. Our study provided imaging evidence that bone formation is involved in the pathogenesis of multiple PsA domains. However, the clinical application of ^{18}F-NaF-PET has been examined in metabolic, autoimmune, and osteogenic bone disorders. Therefore, in addition to the specific lesions of PsA, other pathological bone diseases like degenerative lesions can also show positive ^{18}F-NaF uptake [28]. Future research should focus on differentiation between typical PsA and degenerative lesions.

We found that ^{18}F-NaF PET/CT had a higher positivity rate than ^{68}Ga-FAPI PET/CT in the peripheral, enthetic and axial joints of PsA patients. The different uptake patterns suggest that these radiotracers are related to different aspects of PsA pathogenesis. Bone formation, enthesitis, and axial arthritis are associated, which may explain the higher ^{18}F-NaF than ^{68}Ga-FAPI tracer uptake in the entheses and axial joints [29, 30]. In addition, osteoclastogenesis-supporting fibroblasts are present in the synovia, and synovial fibroblasts were found to express high RANKL levels, which is important for osteoclast differentiation [31, 32]. This suggests that the immune system induces osteoclastogenesis by stimulating synovial fibroblasts. Lories *et al.* demonstrated high BMP-2 and -6 levels in synovial fibroblasts and macrophages in synovial biopsies of patients with AS, and BMP/TGF-β were involved in the pathogenesis of enhanced bone formation. We speculate that ^{68}Ga-FAPI enhancement occurs at the stage of synovial fibroblast activation, while ^{18}F-NaF uptake lasts even after arthritis subsides. We propose that ^{68}Ga-FAPI PET/CT could help to distinguish the actual disease activity from irreversible joint damage. The correlation between PET joint count and PASDAS further supports this idea. Future studies should compare the clinical significance of both radiotracers to establish their roles in PsA.

The PET/CT findings and clinical assessments differed for PsA in the present study. Since ^{18}F-NaF PET/CT can visualize new molecular bone formation and ^{68}Ga-FAPI PET/CT can detect activated synovial fibroblasts in early subclinical stages, such differences between PET-CT and clinical findings may be anticipated. In addition, axial involvement in this study was defined based on imaging (X-ray, CT), although history of inflammatory back pain was collected for each patient. Therefore, the results may not be pertinent to non-radiographic PsA. In addition, PET-positive but US-negative joints and entheses were observed, for two possible reasons. We initially thought that hypermetabolic joints with a normal US appearance might be joints with an inflammatory component without proliferating synovitis; thus, the sensitivity of the metabolic measurements for identifying subclinical joint inflammation using ^{68}Ga-FAPI PET/CT was higher. ^{18}F-NaF PET/CT visualizes new bone formation, and thus can even detect ongoing bone destruction, whereas US primarily images inflammatory activity. Bone remodelling has been demonstrated in the entheses and MCP joints of patients with psoriasis without clinically diagnosed PsA [33]. Additionally, several studies have suggested highly sensitive detection of subclinical disease activity by ^{18}F-NaF PET/CT, which may precede PsA radiological abnormalities. An alternative explanation is that these reflected false-positive PET/CT results. These joints may develop secondary OA. Imaging studies using different methods are required for future pathogenic research.

The limitations of this study are as follows. First, this study was performed in a small group of patients with PsA, and we did not evaluate dactylitis or nail pathology. The values of some ROC analyses were difficult to interpret due to the small sample size. Furthermore, in this pilot study, participants with not only moderate or high disease activity (9 patients based on PASDAS), but also low disease activity or remission (7 patients) were enrolled, resulting in the low positivity rates detected by PET-CT. Further studies with a larger sample size should be conducted. Second, this study lacked controls with other forms of arthritis. Additional studies should investigate a variety of patients with other forms of inflammatory arthritis. Third, the two readers did not read the images independently but worked together and reached a consensus for PET/CT interpretation, which may have potentially biased the result. Fourth, we did not consider the presence of structural damages caused by degenerative change (secondary OA), because it is difficult to determine the pathology on the basis of the finding of PET/CT alone. Fifth, intrascan motion lasts 20 min, which may involve a somewhat blurring in the peripheral joints. However, a low-dose CT scan, which was used to obtain a precise localization of the lesion, was performed prior to each PET scan, and patients were asked to stay motionless before examination. Another concern is radiation exposure. Although MRI is the standard modality used in some contexts (axial inflammation, peripheral arthritis, enthesitis), an unenhanced low-dose CT protocol which used both for attenuation correction and anatomic reference could limit the radiation exposure. In this study, the effective dose of ^{18}F-NaF PET/CT was varied from 6 to 14 mSv (4–10 mSv from the PET tracer and 2–4 mSv from the low-dose CT scan), and ^{68}Ga-FAPI PET/CT has an estimated dose of 5.3 mSv (1.56 ± 0.26 mSv from the PET tracer and 3.7 mSv from the low-dose CT scan). Finally, the heterogeneity of the PET/CT protocols (eg. uptake time, dose, use of two different PET/CT scanners and

reconstruction parameters) in our study may have biased the measurements.

In summary, the positivity rates of ^{68}Ga-FAPI and ^{18}F-NaF PET/CT differed in the peripheral joints, entheses, and axial joints of patients with PsA. In ^{68}Ga-FAPI PET/CT, the positivity rate was higher in the peripheral joints than in the entheses and axial joints, whereas in ^{18}F-NaF PET/CT, the positivity rates in all three domains were high. The extent of joint involvement as shown in ^{68}Ga-FAPI PET/CT was correlated with clinical and US variables as well as disease activity. The different uptake patterns revealed that these two radiotracers were related to different aspects of pathogenesis in PsA. Further studies are warranted to clarify the roles of FAP and bone metabolism in PsA. In addition, there have been numerous studies about ^{18}F-FDG PET/CT in PsA. In the future, add ^{18}F-FDG could be added for comparison, to better understand the role of ^{68}Ga-FAPI PET/CT in PsA assessment.

Supplementary material

Supplementary material is available at *Rheumatology* online.

Data availability

The datasets used and/or analysed during the current study are available from the corresponding author on reasonable request.

Funding

This study was supported by the National Basic Research Program of China (973 Program) (No. 2014CB541801).

Disclosure statement: The authors have declared no conflicts of interest.

Acknowledgements

The authors would like to thank all the patients and clinicians and radiologists who contributed to the present study.

References

1. Ritchlin CT, Colbert RA, Gladman DD. Psoriatic arthritis. N Engl J Med 2017;376:957–70.
2. Veale DJ, Fearon U. The pathogenesis of psoriatic arthritis. Lancet 2018;391:2273–84.
3. Poddubnyy D, Jadon DR, Van den Bosch F, Mease PJ, Gladman DD. Axial involvement in psoriatic arthritis: an update for rheumatologists. Semin Arthritis Rheum 2021;51:880–7.
4. Leung YY, Ogdie A, Orbai A-M *et al.* Classification and outcome measures for psoriatic arthritis. Front Med (Lausanne) 2018;5:246.
5. Coates LC, Hodgson R, Conaghan PG, Freeston JE. MRI and ultrasonography for diagnosis and monitoring of psoriatic arthritis. Best Pract Res Clin Rheumatol 2012;26:805–22.
6. van der Krogt JMA, van Binsbergen WH, van der Laken CJ, Tas SW. Novel positron emission tomography tracers for imaging of rheumatoid arthritis. Autoimmun Rev 2021;20:102764.
7. Bauer S, Jendro MC, Wadle A *et al.* Fibroblast activation protein is expressed by rheumatoid myofibroblast-like synoviocytes. Arthritis Res Ther 2006;8:R171.
8. Croft AP, Campos J, Jansen K *et al.* Distinct fibroblast subsets drive inflammation and damage in arthritis. Nature 2019; 570:246–51.
9. Laverman P, van der Geest T, Terry SYA *et al.* Immuno-PET and immuno-SPECT of rheumatoid arthritis with radiolabeled anti-fibroblast activation protein antibody correlates with severity of arthritis. J Nucl Med 2015;56:778–83.
10. van der Geest T, Roeleveld DM, Walgreen B *et al.* Imaging fibroblast activation protein to monitor therapeutic effects of neutralizing interleukin-22 in collagen-induced arthritis. Rheumatology (Oxford) 2018;57:737–47.
11. Luo Y, Pan Q, Zhou Z *et al.* (68)Ga-FAPI PET/CT for rheumatoid arthritis: a prospective study. Radiology 2023;307:e222052.
12. Schmidkonz C, Rauber S, Raimondo MG *et al.* Fibroblast activation protein (FAP) PET-CT imaging allows to depict inflammatory joint remodeling in patients with psoriatic arthritis. Ann Rheum Dis 2022;81:169.
13. Grant FD, Fahey FH, Packard AB *et al.* Skeletal PET with 18F-fluoride: applying new technology to an old tracer. J Nucl Med 2008;49:68–78.
14. Paine A, Ritchlin C. Bone remodeling in psoriasis and psoriatic arthritis: an update. Curr Opin Rheumatol 2016;28:66–75.
15. Watanabe T, Takase-Minegishi K, Ihata A *et al.* (18)F-FDG and (18)F-NaF PET/CT demonstrate coupling of inflammation and accelerated bone turnover in rheumatoid arthritis. Mod Rheumatol 2016;26:180–7.
16. de Jongh J, Hemke R, Zwezerijnen GJC *et al.* (18)F-sodium fluoride PET-CT visualizes both axial and peripheral new bone formation in psoriatic arthritis patients. Eur J Nucl Med Mol Imaging 2023;50:756–64.
17. Helliwell PS, Taylor WJ. Classification and diagnostic criteria for psoriatic arthritis. Ann Rheum Dis 2005;64 Suppl 2:ii3–8.
18. Ficjan A, Husic R, Gretler J *et al.* Ultrasound composite scores for the assessment of inflammatory and structural pathologies in Psoriatic Arthritis (PsASon-Score). Arthritis Res Ther 2014; 16:476.
19. de Miguel E, Cobo T, Muñoz-Fernández S *et al.* Validity of enthesis ultrasound assessment in spondyloarthropathy. Ann Rheum Dis 2009;68:169–74.
20. Luo Y, Pan Q, Yang H *et al.* Fibroblast activation protein-targeted PET/CT with (68)Ga-FAPI for imaging IgG4-related disease: comparison to (18)F-FDG PET/CT. J Nucl Med 2021; 62:266–71.
21. Abdelhafez Y, Raychaudhuri SP, Mazza D *et al.* Total-Body (18)F-FDG PET/CT in autoimmune inflammatory arthritis at ultra-low dose: initial observations. J Nucl Med 2022;63:1579–85.
22. Dendl K, Koerber SA, Kratochwil C *et al.* FAP and FAPI-PET/CT in malignant and non-malignant diseases: a perfect symbiosis? Cancers 2021;13:4946.
23. Dorst DN, Rijpkema M, Buitinga M *et al.* Targeting of fibroblast activation protein in rheumatoid arthritis patients: imaging and ex vivo photodynamic therapy. Rheumatology (Oxford) 2022; 61:2999–3009.
24. Fromm S, Cunningham CC, Dunne MR *et al.* Enhanced angiogenic function in response to fibroblasts from psoriatic arthritis synovium compared to rheumatoid arthritis. Arthritis Res Ther 2019;21:297.
25. Yao L, Zhao L, Pang Y, Shang Q, Chen H. Increased 68Ga-FAPI uptake in ankylosing spondylitis in a patient with rectal cancer. Clin Nucl Med 2022;47:176–8.
26. McGonagle D. Imaging the joint and enthesis: insights into pathogenesis of psoriatic arthritis. Ann Rheum Dis 2005;64(Suppl 2):ii58–60.
27. Appel H, Ruiz-Heiland G, Listing J *et al.* Altered skeletal expression of sclerostin and its link to radiographic progression in ankylosing spondylitis. Arthritis Rheum 2009;60:3257–62.
28. Park PSU, Raynor WY, Sun Y *et al.* 18F-sodium fluoride PET as a diagnostic modality for metabolic, autoimmune, and osteogenic bone disorders: cellular mechanisms and clinical applications. Int J Mol Sci 2021;22:6504.
29. Araujo EG, Schett G. Enthesitis in psoriatic arthritis (Part 1): pathophysiology. Rheumatology (Oxford) 2020;59:i10–i14.

30. Sieper J, Poddubnyy D. Axial spondyloarthritis. Lancet 2017; 390:73–84.
31. Takayanagi H, Iizuka H, Juji T *et al.* Involvement of receptor activator of nuclear factor kappaB ligand/osteoclast differentiation factor in osteoclastogenesis from synoviocytes in rheumatoid arthritis. Arthritis Rheum 2000;43:259–69.
32. Gravallese EM, Manning C, Tsay A *et al.* Synovial tissue in rheumatoid arthritis is a source of osteoclast differentiation factor. Arthritis Rheum 2000;43:250–8.
33. Simon D, Faustini F, Kleyer A *et al.* Analysis of periarticular bone changes in patients with cutaneous psoriasis without associated psoriatic arthritis. Ann Rheum Dis 2016;75:660–6.

Rheumatology, 2024, 00, 1–8
https://doi.org/10.1093/rheumatology/keae577
Original Article